CMS Physics Analysis Summary

Contact: cms-pag-conveners-susy@cern.ch 2013/08/30

Search for electroweak production of charginos and neutralinos in final states with a Higgs boson in pp collisions at $\sqrt{s} = 8$ TeV

The CMS Collaboration

Abstract

This note reports the results for searches for the direct electroweak production of supersymmetric charginos and neutralinos in final states with a Higgs boson. The data sample consists of pp collisions at a center-of-mass energy $\sqrt{s} = 8$ TeV collected by the CMS experiment at the LHC, corresponding to an integrated luminosity of 19.5 fb^{-1}. The signature consists of a chargino-neutralino pair decaying to a W boson, a Higgs boson, and missing transverse energy from escaping lightest supersymmetric particles. The data are consistent with the standard model backgrounds. The results are interpreted to probe charginos and neutralinos with masses up to 204 GeV.

1 Introduction

Supersymmetry (SUSY) is a popular extension to the standard model (SM) that may alleviate the gauge hierarchy problem, lead to the unification of gauge couplings, and provide a candidate particle for the dark matter [1–6]. Many searches for SUSY performed at the LHC have focused on the strong production of gluinos and squarks, the SUSY partners of the gluon and quarks [7–10]. Null results in these searches probe strongly-interacting SUSY particles up to a mass scale of $\sim$1 TeV. If the squarks and gluinos are heavy, direct electroweak production of charginos and neutralinos, the SUSY partners of the W, Z, and Higgs bosons, may dominate at the LHC. Searches for these particles have also been performed [11, 12]. Due to the smaller electroweak production cross sections, the constraints on the masses of these particles are significantly weaker, up to a few hundred GeV.

The recent observation of a Higgs boson [13, 14] offers the novel possibility to perform beyond-the-SM searches by exploiting the measured properties of this particle. In particular, in large regions of SUSY parameter space the heavy neutralinos are expected to decay predominantly to a Higgs boson, and in this note we report searches for such decays. The data sample consists of pp collisions collected at a center-of-mass energy $\sqrt{s} = 8$ TeV by the CMS experiment at the LHC, corresponding to an integrated luminosity of $19.5\,\text{fb}^{-1}$.

The electroweak SUSY process with the largest cross section is chargino-neutralino pair production. This process has been probed in previous CMS searches [11, 12], which required that the chargino decays to a W boson and the lightest SUSY particle (LSP), assumed to be the lightest neutralino $\tilde{\chi}^0_1$, and that the neutralino decays to a Z boson and the LSP. Here we search for chargino-neutralino pair production where the neutralino decays instead to a Higgs boson and the LSP, $\tilde{\chi}^\pm_1\tilde{\chi}^0_2 \to (\mathrm{W}^\pm\tilde{\chi}^0_1)(\mathrm{H}\tilde{\chi}^0_1)$, as depicted in Fig. 1. The decays $\tilde{\chi}^\pm_1 \to \mathrm{W}^\pm\tilde{\chi}^0_1$ and $\tilde{\chi}^0_2 \to \mathrm{H}\tilde{\chi}^0_1$ are expected to dominate if the $\tilde{\chi}^\pm_1$ and $\tilde{\chi}^0_2$ particles are wino-like, the $\tilde{\chi}^0_1$ is bino-like, and the difference between their masses is larger than $M_\mathrm{H} = 126\,\text{GeV}$. The wino-like nature of the $\tilde{\chi}^\pm_1$ and $\tilde{\chi}^0_2$ particles motivates the simplifying assumption $M_{\tilde{\chi}} \equiv M_{\tilde{\chi}^\pm_1} = M_{\tilde{\chi}^0_2}$. Here the H particle is the lightest SUSY Higgs boson, which is expected to be SM-like if the other SUSY Higgs bosons are significantly heavier than M_Z [15].

Three exclusive final states sensitive to the process in Fig. 1 are considered in this note. In all searches, the W is required to decay leptonically and the $\tilde{\chi}^0_1$ is assumed to be stable and escape detection, leading to large missing transverse energy ($E_\mathrm{T}^\mathrm{miss}$). A search performed in the single lepton final state provides sensitivity to events in which the Higgs boson decays as $\mathrm{H} \to \mathrm{b\bar{b}}$. A search in the same-sign dilepton final state targets events with the decay $\mathrm{H} \to \mathrm{W^+W^-}$ in which one of the W bosons decays leptonically and the other hadronically. The results of the CMS inclusive multi-lepton search [16] are reinterpreted, targeting the decays $\mathrm{H} \to \mathrm{W^+W^-}$, $\mathrm{H} \to \mathrm{ZZ}$, and $\mathrm{H} \to \tau^+\tau^-$. The results from these searches are combined to place limits on the topology of Fig. 1.

2 Simulated samples

Monte Carlo (MC) simulations of signal and SM processes are used to design the analysis, to estimate some of the backgrounds, and to calculate the signal acceptance in the search regions. Event samples for SM processes are generated using the PYTHIA 6.4.22 [17], MADGRAPH 5.1.3.30 [18], MC@NLO [19, 20], or POWHEG [21] MC event generators and the CTEQ6L1 or CTEQ6M parton density functions [22]. All SM processes are normalized to cross section calculations at next-to-leading order (NLO) or next-to-next-to-leading order (NNLO) when available [19, 20, 23–28] and otherwise leading order (LO).

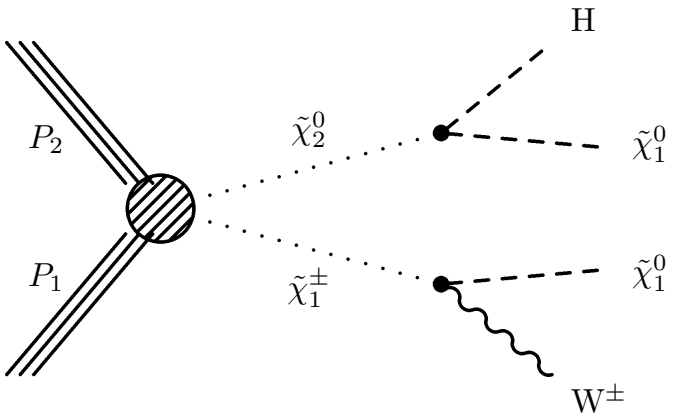

Figure 1: The signal topology targeted in this note: chargino-neutralino pair production leading to the WH + E_T^{miss} final state.

For the signal events, the files specifying the SUSY signal model parameters are generated according to the SUSY Les Houches accord [29] standards with the SuSpect v2.4.1 [30] program. The production of chargino-neutralino pairs is generated with MADGRAPH 5.1.5.4, including up to two additional partons at the matrix-element level. The chargino and neutralino are decayed using BRIDGE v2.24 [31]. Expected signal event rates are normalized to cross sections calculated at NLO [32–34].

In the MC samples, for both signal and backgrounds, multiple proton-proton interactions in the same or nearby bunch crossings (pileup) are simulated using PYTHIA and superimposed on the hard collision. Simulated events are reweighted to match the pileup distributions in data. The background and signal yields from MC simulations are corrected for differences in measured efficiencies between data and simulation.

The simulation of new physics signals is performed using the CMS fast simulation package [35], while the SM samples are simulated using a GEANT4-based model [36] of the CMS detector. The simulated events are finally reconstructed and analyzed with the same software used to process collision data.

3 Event selection

Events from pp interactions must satisfy the requirements of a two-level trigger system. The first level performs a fast selection of physics objects (jets, muons, electrons, and photons) above certain thresholds. The second level performs a full event reconstruction. The principal triggers used for these analyses require the presence of a $p_T > 27\,GeV$ (24 GeV) electron (muon), or a pair of leptons (ee, eμ, or $\mu\mu$) with leading $p_T > 17\,GeV$ and trailing $p_T > 8\,GeV$.

Events are reconstructed offline using the particle-flow (PF) algorithm [37, 38], which provides a self-consistent global assignment of momenta and energies to the physics objects. Details of the reconstruction and identification procedures are given in Refs. [39, 40] for electrons and muons. Jets are reconstructed with the anti-k_T clustering algorithm [41] with a distance parameter of 0.5. We apply p_T- and η-dependent corrections to the jet momentum to account for residual effects of non-uniform detector response. The contribution to jet energy from pileup is estimated on an event-by-event basis using the jet area method described in Ref. [42], and

is subtracted from the overall jet p_T. We reject jets that are consistent with anomalous noise in the calorimeter detectors. Jets are required to be consistent with originating from the signal primary vertex, to suppress jets from pileup events.

Lepton (e, μ) candidates are required to be consistent with originating from the primary vertex. To reduce contamination from leptons from heavy-flavor decay or misidentified hadrons in jets, leptons are required to be isolated and to have a transverse impact parameter with respect to the primary vertex satisfying $d_0 < 0.2$ mm. Electron and muon candidates are considered isolated if the ratio of the scalar sum of the transverse momenta of charged hadrons, photons, and neutral hadrons in a cone of $\Delta R = \sqrt{\Delta\eta^2 + \Delta\phi^2} = 0.3$ around the candidate, relative to the lepton p_T value, is less than 0.15. The isolation is corrected for the expected contribution from pileup events. Standard electron and muon quality criteria are imposed [39, 40].

Hadronic decays of the τ lepton are reconstructed using the "hadrons-plus-strips"algorithm [43], which combines PF photon and electron candidates to form neutral pions. The neutral pions are combined with charged hadrons to form hadronic τ decay candidates.

Jets must satisfy $|\eta| < 2.5$ and $p_T > 30$ GeV and be separated by $\Delta R > 0.4$ from candidate leptons. Jets originating from b quarks (b-jets) are identified using the Combined Secondary Vertex loose, medium, or tight (CSVL, CSVM, CSVT) working points [44]. The E_T^{miss} is defined as the modulus of the vector sum of the transverse momenta of all PF objects.

Some of the searches make use of the transverse mass of the lepton-E_T^{miss} system, defined as $M_T = \sqrt{2p_T^{\ell}E_T^{miss}(1-\cos(\phi))}$, where ϕ is the angle between the transverse momentum of the lepton and E_T^{miss} and p_T^{ℓ} is the transverse momentum of the electron or muon.

4 Search in the single-lepton final state

4.1 Overview of search

In this section we report the results from a search for $\tilde{\chi}_1^{\pm}\tilde{\chi}_2^0 \to (W\tilde{\chi}_1^0)(H\tilde{\chi}_1^0) \to \ell\nu b\bar{b} + E_T^{miss}$. The Higgs boson decay mode $H \to b\bar{b}$ has the largest branching fraction (56%). Searches for the SM Higgs boson decaying to a pair of b-quarks have targeted the associated production with a leptonically-decaying W boson [45]. In this search, we impose additional kinematic requirements on E_T^{miss} and other related quantities which strongly suppress both the SM backgrounds and the SM production of a Higgs boson, while retaining efficiency for the SUSY signal.

This search is an extension of the search for direct top squark pair production [46], which targets events with a single lepton, (b-tagged) jets, and E_T^{miss}, with similar object selection and analysis methodology. The final state considered here is similar, except that we expect two fewer jets.

Events are selected containing a single lepton, two b-tagged jets, and E_T^{miss}. The largest backgrounds come from $t\bar{t}$ production, both semi-leptonic $t\bar{t}$ and dilepton $t\bar{t}$ where the second lepton is not identified. Production of W + jets also constitutes an important background. The SM backgrounds are suppressed using several kinematic requirements which exploit the extra E_T^{miss} in signal events from the invisible LSPs. Signal regions are defined by successively tighter requirements on E_T^{miss}, and counting experiments are performed. The signal is expected to produce a bump in the dijet mass spectrum at $M_{b\bar{b}} = M_H$.

Most of the SM backgrounds are estimated from simulation, with the exception of W+light jets, which is extrapolated from control regions in data. Scale factors and corresponding uncertainties on the predictions from simulation are assessed based on comparisons to data in control

regions.

4.2 Event selection

Signal events are collected with inclusive single lepton triggers. Dilepton triggers are used to select events in the dilepton control region, described below.

We select events with exactly one high p_T electron or muon, requiring lepton $p_T > 30(25)$ GeV and $|\eta| < 1.4442(2.1)$ for electrons (muons). We require exactly two jets in the event within $|\eta| < 2.4$, and the leading jet must satisfy $p_T > 50$ GeV. A further jet veto is imposed, requiring exactly two jets counted in the range $|\eta| < 4.7$. This substantially reduces the $t\bar{t} \to \ell +$ jets background, which typically has four jets. The two selected jets must satisfy the CSVM b-tagging requirement.

The extra E_T^{miss} from the LSPs is one of the best handles to discriminate against the SM background. The analysis preselection requires $E_T^{miss} > 50$ GeV, while the signal regions vary the threshold from 100 to 175 GeV. We require $M_T > 100$ GeV, which primarily rejects backgrounds with a single $W \to \ell\nu$ and no additional E_T^{miss}: $t\bar{t} \to \ell +$ jets, W + jets, and single top t- and s-channel, as well as SM $WH \to \ell\nu b\bar{b}$.

To suppress the dilepton $t\bar{t}$ backgrounds, events with an indication of a second lepton (i.e. an isolated track or hadronic τ candidate) are rejected.

Further suppression of the $t\bar{t}$ backgrounds is achieved with the M_{T2}^{bl} variable [47]. The M_{T2}^{bl} quantity is defined as the minimum "mother" particle mass compatible with the 4-momenta of the lepton, b-tagged jets, and E_T^{miss}. It has an endpoint at M_{top} for $t\bar{t}$ events without mismeasurement effects, while signal events may have larger values. We require $M_{T2}^{bl} > 200$ GeV.

The dijet mass $M_{b\bar{b}}$ is formed from the two selected jets. For the signal region, a dijet mass window around the Higgs boson mass is imposed: $100 < M_{b\bar{b}} < 150$ GeV. This requirement has an efficiency of about 80% for signal events.

4.3 Backgrounds and estimation methodology

Backgrounds are grouped into six categories. The largest background is from $t\bar{t}$ events and single top production in the tW channel, in which both W bosons decay leptonically (dilepton top background). Backgrounds from $t\bar{t}$ and single top with one leptonically-decaying W boson are referred to as the single lepton top background. Backgrounds from WZ production, where the W boson decays leptonically and the Z boson decays to a $b\bar{b}$ pair are referred to as the $WZ \to \ell\nu b\bar{b}$ background. Backgrounds from W bosons produced in association with b-quarks are referred to as the $W + b\bar{b}$ background, while production of W bosons with other partons constitutes the W+light jets background. Finally, the "rare backgrounds" consist of processes with two top quarks and a vector boson, diboson, triboson, Z + jets, and also SM $WH \to \ell\nu b\bar{b}$. The Z + jets process has a large cross section but is included in the rare category because it is very small after the signal region requirements are imposed. With the exception of the W+light jets background, background estimation is based on simulation.

The simulation is validated in three data control regions that are enriched in different backgrounds. A data sample enriched in W+light jets is defined by vetoing events with b-tagged jets (CR-0b). A data sample enriched in the dilepton top background is defined by requiring either exactly two leptons satisfying the analysis selection, or one such lepton and an isolated track (CR-2ℓ). Finally, the $M_{b\bar{b}}$ requirement is inverted to obtain a data sample (CR-$M_{b\bar{b}}$) consisting of a mixture of backgrounds with similar composition as the signal region.

The agreement between the data and the simulation in the three data control regions is used to assess scale factors and uncertainties on the background predictions. In CR-2ℓ, the data are found to be in good agreement with the predictions from simulation, which are dominated by the dilepton top background. A 40% uncertainty is assessed on the dilepton top background, based on the limited statistical precision of the event sample after applying all the kinematical requirements. Correction factors of 0.8 ± 0.3, 1.2 ± 0.5 and 1.0 ± 0.6 are assessed on the WZ $\to \ell\nu\mathrm{b\bar{b}}$, $\mathrm{W} + \mathrm{b\bar{b}}$, and single lepton top backgrounds, respectively, based on studies of CR-$M_{\mathrm{b\bar{b}}}$ and CR-0b. The rare backgrounds are estimated from simulation with a 50% systematic uncertainty.

The W+light jets background prediction is extrapolated from CR-0b, using the b-tagging misidentification rate for light flavor jets measured from simulation. This rate includes all flavors except b-quarks. The uncertainty is 40%, due to uncertainties in the b-tagging misidentification rate and its variation with respect to the jet p_{T}.

4.4 Results

Four signal regions are defined by the requirements $E_{\mathrm{T}}^{\mathrm{miss}} > 100, 125, 150, 175\,\mathrm{GeV}$. In general, signal regions with tighter $E_{\mathrm{T}}^{\mathrm{miss}}$ requirements are more sensitive to signal models with larger mass differences $M_{\tilde{\chi}} - M_{\tilde{\chi}_1^0}$. The results in these signal regions are summarized in Table 1. Good agreement is observed between the data and the background predictions. The expected signal yields for several model points are also indicated, including systematic uncertainties that are discussed in Sec. 7. The distributions of $M_{\mathrm{b\bar{b}}}$ are displayed in Fig. 2, after all selection requirements except that on $M_{\mathrm{b\bar{b}}}$. No evidence for a peak at $M_{\mathrm{b\bar{b}}} = M_{\mathrm{H}}$ is observed.

Table 1: Summary of results for the single lepton analysis. The expected background contributions are compared to the observed yields in data for the four signal regions. The expectations from a few signal points are indicated; the first number indicates $M_{\tilde{\chi}}$ and the second number indicates $M_{\tilde{\chi}_1^0}$. The uncertainties that are shown contain statistical and systematic uncertainties.

Sample	$E_{\mathrm{T}}^{\mathrm{miss}} > 100$ GeV	$E_{\mathrm{T}}^{\mathrm{miss}} > 125$ GeV	$E_{\mathrm{T}}^{\mathrm{miss}} > 150$ GeV	$E_{\mathrm{T}}^{\mathrm{miss}} > 175$ GeV
Dilepton top	2.8 ± 1.2	2.3 ± 1.0	1.7 ± 0.7	1.2 ± 0.5
Single lepton top	1.8 ± 1.1	0.9 ± 0.6	0.5 ± 0.3	0.2 ± 0.2
WZ $\to \ell\nu\mathrm{b\bar{b}}$	0.6 ± 0.2	0.4 ± 0.2	0.3 ± 0.1	0.3 ± 0.1
$\mathrm{W} + \mathrm{b\bar{b}}$	1.5 ± 0.9	1.0 ± 0.7	0.9 ± 0.6	0.2 ± 0.3
W+light jets	0.5 ± 0.2	0.3 ± 0.1	0.2 ± 0.1	0.2 ± 0.1
Rare	0.4 ± 0.2	0.3 ± 0.2	0.3 ± 0.2	0.2 ± 0.1
Total SM	7.7 ± 1.9	5.4 ± 1.3	3.8 ± 1.0	2.3 ± 0.6
Data	7	6	3	3
$\tilde{\chi}_1^\pm\tilde{\chi}_2^0 \to (\mathrm{W}\tilde{\chi}_1^0)(\mathrm{H}\tilde{\chi}_1^0)$ (130/1)	9.0 ± 1.2	7.5 ± 1.0	6.0 ± 0.8	4.5 ± 0.6
$\tilde{\chi}_1^\pm\tilde{\chi}_2^0 \to (\mathrm{W}\tilde{\chi}_1^0)(\mathrm{H}\tilde{\chi}_1^0)$ (150/1)	7.3 ± 1.0	6.2 ± 0.9	5.0 ± 0.7	3.6 ± 0.5
$\tilde{\chi}_1^\pm\tilde{\chi}_2^0 \to (\mathrm{W}\tilde{\chi}_1^0)(\mathrm{H}\tilde{\chi}_1^0)$ (200/1)	7.3 ± 1.0	6.0 ± 0.8	4.9 ± 0.7	3.6 ± 0.5
$\tilde{\chi}_1^\pm\tilde{\chi}_2^0 \to (\mathrm{W}\tilde{\chi}_1^0)(\mathrm{H}\tilde{\chi}_1^0)$ (300/1)	5.5 ± 0.7	5.2 ± 0.7	4.6 ± 0.6	4.1 ± 0.6
$\tilde{\chi}_1^\pm\tilde{\chi}_2^0 \to (\mathrm{W}\tilde{\chi}_1^0)(\mathrm{H}\tilde{\chi}_1^0)$ (400/1)	3.4 ± 0.4	3.3 ± 0.4	3.0 ± 0.4	2.7 ± 0.4

5 Search in the same-sign dilepton final state

5.1 Overview of search

In this section we report the results from a search in the same-sign (SS) dilepton final state that is sensitive to $\mathrm{WH} + E_{\mathrm{T}}^{\mathrm{miss}}$ signal events with $\mathrm{H} \to \mathrm{W}^+\mathrm{W}^-$, in which one of the W bosons from the Higgs boson decays leptonically and the other hadronically. The object selections and background estimation methodology follow those in the inclusive same-sign dilepton search [48].

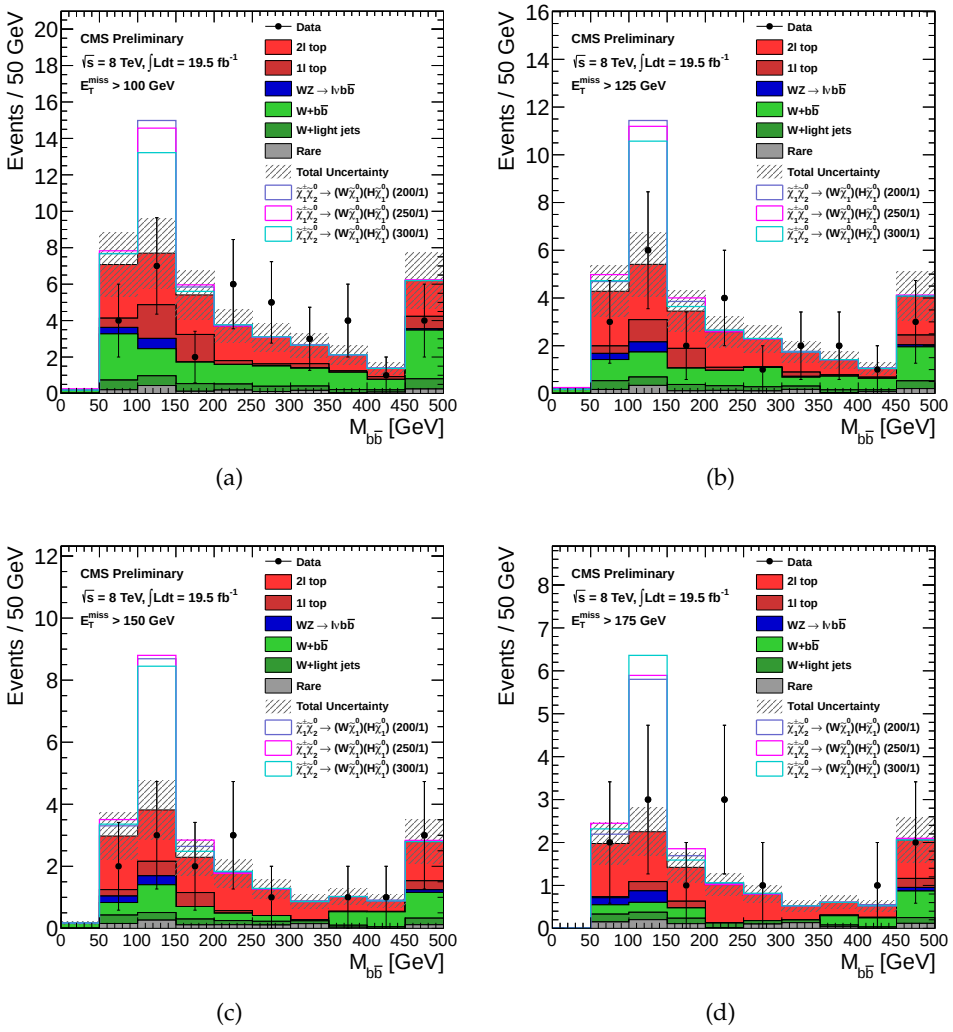

Figure 2: The distributions of $M_{\mathrm{b\bar{b}}}$ for the signal regions with (a) $E_{\mathrm{T}}^{\mathrm{miss}} > 100\,\mathrm{GeV}$, (b) $E_{\mathrm{T}}^{\mathrm{miss}} > 125\,\mathrm{GeV}$, (c) $E_{\mathrm{T}}^{\mathrm{miss}} > 150\,\mathrm{GeV}$, and (d) $E_{\mathrm{T}}^{\mathrm{miss}} > 175\,\mathrm{GeV}$. The data are compared to the sum of the expected backgrounds. Three sample signal model points are also indicated, stacked on top of the SM background. The uncertainty band includes the statistical and systematic uncertainty on the background prediction.

Events with SS leptons, jets, and moderate $E_{\mathrm{T}}^{\mathrm{miss}}$ are selected. Backgrounds with fake leptons and electrons with mismeasured charge are estimated from control regions in data, while backgrounds from muons with mismeasured charge are negligible. Here, fake lepton can refer to a lepton from a heavy flavor decay, decay-in-flight, or a misidentified jet. Additional backgrounds from a variety of SM processes with genuine SS leptons are estimated from simulation. Processes yielding a real same-sign lepton pair account for slightly more than half of the expected background, with the remainder from processes containing a fake electron or muon. The background from processes containing an electron with mis-reconstructed charge is very small.

The most sensitive variable for this search, $M_{\ell\mathrm{jj}}$, attempts to reconstruct the Higgs boson mass from the W daughters by taking the invariant mass of the lepton-dijet system formed by the two highest p_{T} jets and the lepton closest to the dijet axis. The signal would present itself as

a peak below M_{H}, due to the missing ν, while the backgrounds tend to have larger values, as indicated in Fig. 3. A signal region is defined by requiring low $M_{\ell\mathrm{jj}}$ in addition to other kinematical requirements designed to suppress the SM backgrounds, and a counting experiment is performed.

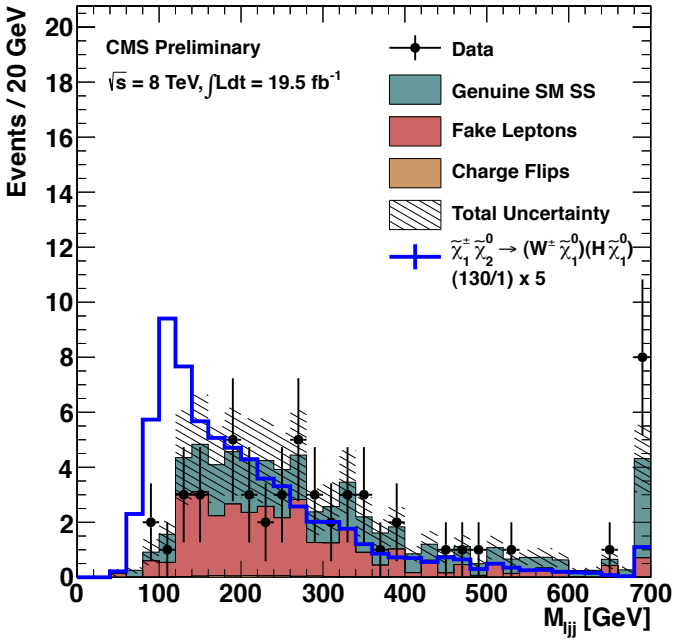

Figure 3: The observed $M_{\ell\mathrm{jj}}$ distribution, compared to the sum of the expected backgrounds, after all selection requirements except that on $M_{\ell\mathrm{jj}}$. An example signal model point with $M_{\tilde{\chi}} = 130\,\mathrm{GeV}$ and $M_{\tilde{\chi}_1^0} = 1\,\mathrm{GeV}$ is overlaid. The signal normalization has been scaled up by a factor of 5 relative to the theory prediction.

5.2 Event selection

We require the presence of exactly two e or μ leptons (ee, $\mu\mu$, or eμ) with the same sign. The leptons must satisfy $p_{\mathrm{T}} > 20\,\mathrm{GeV}$. Due to the large background from fake leptons, the d_0 and isolation criteria are tighter in this search than in the others presented in this note. Background from electron charge mismeasurement is reduced by requiring consistency among three independent measurements of the electron charge.

We require the presence of two or three $p_{\mathrm{T}} > 30$ GeV jets. Due to the background suppression provided by the requirement of two same-sign leptons, we are able to relax the $E_{\mathrm{T}}^{\mathrm{miss}}$ requirement with respect to the single lepton search, and we require $E_{\mathrm{T}}^{\mathrm{miss}} > 40\,\mathrm{GeV}$. Events with a b-tagged jet (using CSVT) are vetoed, as are events with two or more CSVL b-tagged jets. These two vetoes suppress background from events containing top quarks. Events with a third lepton, defined as an identified e, μ, or hadronic τ candidate, are vetoed to suppress backgrounds coming from the SM production of final states containing multiple electroweak bosons.

The transverse mass M_{T} is computed for each of the selected leptons, and at least one lepton must satisfy $M_{\mathrm{T}} > 110$ GeV. This requirement suppresses processes containing a single leptonically decaying W boson, for which the transverse mass distribution has a natural endpoint at the W mass. We additionally require that the separation between the leptons satisfy $\Delta\eta(\ell_1, \ell_2) < 1.6$. Restricting the separation between the leptons suppresses background from

processes with fake leptons as well as the SM production of two quarks together with two W bosons of the same electric charge. We require $M_{T2}^{J} > 100$ GeV for additional rejection of top quark pairs where one W decays to a lepton and a neutrino and a second lepton of the same electric charge arises from the decay of a b-quark. The variable M_{T2}^{J} is similar to the M_{T2}^{bl} variable described in Section 4.2 except that it is computed using both leptons, instead of just one, as well as jets and E_T^{miss} [49, 50]. All jets passing the kinematic requirements are considered in the calculation and the minimum value of M_{T2}^{J} is chosen. Finally, we require $M_{\ell jj} < 120$ GeV. This variable is a proxy for the reconstruction of the Higgs boson mass and thus helps to suppress all sources of SM background.

5.3 Backgrounds and estimation methodology

The SM backgrounds satisfying the above selection can be grouped into three categories. The largest background category includes a variety of SM processes with small cross section, including diboson, triboson, processes with two top quarks and a vector boson, and SM production of two same-sign W bosons. The SM production of a Higgs boson in association with a W boson is also included in this category, although it is negligible in our signal region. These backgrounds are estimated from simulation with a 50% systematic uncertainty.

The second largest category includes processes with at least one fake lepton. This background, dominated by $t\bar{t}$ and $W+$jets processes, is estimated with an extrapolation technique based on the lepton relative isolation. Based on the difference between true and predicted background yields when the method is applied in simulation, a systematic uncertainty of 50% is assessed. This accounts for differences in sample composition and kinematics between the fake lepton background sample and the QCD-enriched control sample used to measure the fake rate [51].

The smallest contribution to the background is from events with an electron with mismeasured charge. This background, sometimes referred to as charge flips, is dominated by $t\bar{t}$ and $Z+$jets processes and is estimated from studies of $Z \to ee$ events in data and simulation. A 30% systematic uncertainty is assigned based on analysis of data control regions and differences between kinematics in Z + jets and $t\bar{t}$ events.

The background estimation methodology is validated in the signal-depleted sideband region defined by inverting the $M_{\ell jj}$ requirement. Here we observe 51 events, which is consistent with the expected background of 62 ± 22 events.

5.4 Results

The results are summarized in Table 2. No evidence for a peak in the $M_{\ell jj}$ distribution is observed, as indicated in Fig. 3. In the signal region with $M_{\ell jj} < 120$ GeV, we observe 3 events and expect 2.9 ± 1.2 SM background events, hence no excess is observed above the expected SM backgrounds.

6 Search in the multi-lepton final state

The signal model of Fig. 1 can produce multi-lepton final states if the Higgs boson decays to WW, ZZ, or $\tau\tau$, followed by leptonic decays of the W or Z boson. Here we reinterpet the experimental results from the inclusive multi-lepton SUSY search [16].

Events with at least three leptons are selected, including up to one hadronic τ candidate. These events are categorized into multiple exclusive signal regions based on the number and flavor of the leptons, the presence or absence of an opposite-sign, same-flavor (OSSF) lepton pair and

Table 2: Summary of results for the same-sign dilepton analysis. The expected background contributions are compared to the observed yields in data. The uncertainties that are shown contain statistical and systematic uncertainties. The expected signal yields in several example model points are also indicated.

Sample	ee	$\mu\mu$	$e\mu$	Total
Fakes	0.3 ± 0.3	0.2 ± 0.2	0.8 ± 0.5	1.3 ± 0.8
Charge Flips	< 0.01	< 0.01	< 0.03	< 0.03
Genuine SM SS	0.4 ± 0.4	0.4 ± 0.4	0.8 ± 0.6	1.6 ± 0.9
Total SM	0.7 ± 0.5	0.6 ± 0.5	1.6 ± 0.7	2.9 ± 1.2
Data	1	1	1	3
$\tilde{\chi}_1^\pm\tilde{\chi}_2^0 \to (W\tilde{\chi}_1^0)(H\tilde{\chi}_1^0)$ (130/1)	0.8±0.1	1.0±0.1	1.9±0.3	3.6±0.5
$\tilde{\chi}_1^\pm\tilde{\chi}_2^0 \to (W\tilde{\chi}_1^0)(H\tilde{\chi}_1^0)$ (150/1)	0.5±0.1	0.6±0.1	1.4±0.2	2.5±0.3
$\tilde{\chi}_1^\pm\tilde{\chi}_2^0 \to (W\tilde{\chi}_1^0)(H\tilde{\chi}_1^0)$ (200/1)	0.20±0.03	0.4±0.1	0.6±0.1	1.2±0.2
$\tilde{\chi}_1^\pm\tilde{\chi}_2^0 \to (W\tilde{\chi}_1^0)(H\tilde{\chi}_1^0)$ (300/1)	0.07±0.01	0.12±0.02	0.19±0.03	0.4±0.1
$\tilde{\chi}_1^\pm\tilde{\chi}_2^0 \to (W\tilde{\chi}_1^0)(H\tilde{\chi}_1^0)$ (400/1)	0.02±0.00	0.03±0.00	0.06±0.01	0.11±0.02

Table 3: Multi-lepton results, along with the number of expected signal events, in the 5 best signal regions for the $M_{\tilde{\chi}} = 130\,\text{GeV}$, $M_{\tilde{\chi}_1^0} = 1\,\text{GeV}$ model point. All signal regions shown have exactly three selected leptons, a veto on b-tagged jets, and $H_\text{T} < 200$ GeV. The results are binned in the number of hadronic τ candidates and the E_T^miss. Above Z (below Z) indicates the presence of an OSSF pair with invariant mass $M_{\ell\ell} > 105$ GeV (< 75 GeV).

N_{τ_had}	OSSF pair	E_T^miss [GeV]	Data	Total SM	Signal
0	below Z	50–100	142	125 ± 28	24.4 ± 4.4
0	below Z	100–150	16	21.3 ± 8.0	6.8 ± 1.2
0	none	0–50	53	52 ± 12	8.7 ± 1.7
0	none	50–100	35	38 ± 15	10.8 ± 2.0
0	none	100–150	7	9.3 ± 4.3	3.37 ± 0.54

its invariant mass, the presence or absence of a b-tagged jet, the E_T^miss, and the scalar sum of the transverse energies of selected jets, H_T . The most sensitive signal regions for this search are those with exactly three leptons, no b-tagged jets, and low H_T .

Backgrounds from dilepton $\text{t}\bar{\text{t}}$ events with fake leptons are estimated from simulation, while additional sources of fake leptons are estimated using a data-driven method. Backgrounds from WZ and ZZ diboson processes are estimated from simulation, with a correction to the E_T^miss resolution based on comparisons to data in control regions.

The data yields in the signal regions are found to be broadly consistent with the expected SM backgrounds. The observed data yields, expected SM backgrounds, and expected signal yields of the five most sensitive signal regions for the $M_{\tilde{\chi}} = 130\,\text{GeV}$, $M_{\tilde{\chi}_1^0} = 1\,\text{GeV}$ model point (where the multi-lepton analysis has the best sensitivity) are indicated in Table 3. Additional signal-depleted regions are used to constrain the backgrounds and associated uncertainties. Similar results tables for other model points are presented in Appendix A.

7 Interpretation of the results

In this section we interpret the results of the searches in the single-lepton final state (Sec. 4), the same-sign dilepton final state (Sec. 5), and the multi-lepton final state (Sec. 6). The results from

the three channels are then combined to improve the sensitivity.

As discussed earlier, the $\tilde{\chi}_1^\pm$ and $\tilde{\chi}_2^0$ particles are assumed to be wino-like and the $\tilde{\chi}_1^0$ is assumed to be bino-like. The branching fractions for the decays $\tilde{\chi}_1^\pm \to \mathrm{W}\tilde{\chi}_1^0$ and $\tilde{\chi}_2^0 \to \mathrm{H}\tilde{\chi}_1^0$ are assumed to be 100%. The Higgs boson has $M_\mathrm{H} = 126$ GeV and SM-like branching fractions; in particular, $\mathcal{B}(\mathrm{H} \to \mathrm{b\bar{b}}) = 0.56$, $\mathcal{B}(\mathrm{H} \to \mathrm{W^+W^-}) = 0.23$, $\mathcal{B}(\mathrm{H} \to \mathrm{ZZ}) = 0.029$, and $\mathcal{B}(\mathrm{H} \to \tau^+\tau^-) = 0.062$.

Results are presented in the plane of the mass of the LSP, $M_{\tilde{\chi}_1^0}$, and the common mass of the $\tilde{\chi}_1^\pm$ and $\tilde{\chi}_2^0$ particles, $M_{\tilde{\chi}}$. We calculate 95% confidence level (CL) upper limits on the production cross section using the LHC-type CL_S method [52–54]. The limits incorporate uncertainties in the signal acceptance and efficiency from lepton identification and isolation efficiencies, trigger efficiency, jet energy scale and resolution, b-tagging efficiency, and initial state radiation [46], as well as the uncertainty on the integrated luminosity.

For the single-lepton search, several signal regions are defined. For each value of $M_{\tilde{\chi}}$ and $M_{\tilde{\chi}_1^0}$, the cross section limits are based on the signal region with the best expected sensitivity. The cross section limits for the same-sign dilepton search are based on the single signal region defined in that analysis, while those for the multi-lepton results are based on multiple exclusive signal regions, including correlations and bin-to-bin migration of events. For the combination, the results in the three channels are considered simultaneously, taking into account uncertainties that are correlated across the channels.

The results in the plane of $M_{\tilde{\chi}_1^0}$ vs. $M_{\tilde{\chi}}$ are presented in Fig. 4. The signal model is excluded over a portion of the parameter space where $M_{\tilde{\chi}} < 204$ GeV and $M_{\tilde{\chi}_1^0} \lesssim 25$ GeV. The individual results from the three channels and their combination are presented as a function of $M_{\tilde{\chi}}$, for a fixed mass $M_{\tilde{\chi}_1^0} = 1$ GeV, in Fig. 5. The multi-lepton search provides the best sensitivity at low $M_{\tilde{\chi}}$ while the single lepton search dominates at high $M_{\tilde{\chi}}$. The same-sign dilepton search contributes to the combination at low $M_{\tilde{\chi}}$. For $M_{\tilde{\chi}_1^0} = 1$ GeV, we probe $M_{\tilde{\chi}}$ up to 204 GeV, compared to an expectation of 236 GeV, based on the theoretical prediction for the cross section less one standard deviation. For $M_{\tilde{\chi}} = 130$ GeV and $M_{\tilde{\chi}_1^0} = 1$ GeV, the observed (expected) limit on the $\tilde{\chi}_1^\pm\tilde{\chi}_2^0$ production cross section is 3.0 pb (2.1 pb), compared to a theoretical prediction of 4.1 ± 0.3 pb. These searches will benefit from larger data samples to be collected at $\sqrt{s} = 14$ TeV after the LHC shutdown period.

8 Conclusions

This note reports the results from searches for chargino-neutralino production decaying to the $\mathrm{WH} + E_\mathrm{T}^\mathrm{miss}$ final state. Searches in the single-lepton, same-sign dilepton, and multi-lepton channels are performed. No excesses above the SM backgrounds are observed. The results are used to place constraints on the masses of charginos and neutralinos up to 204 GeV.

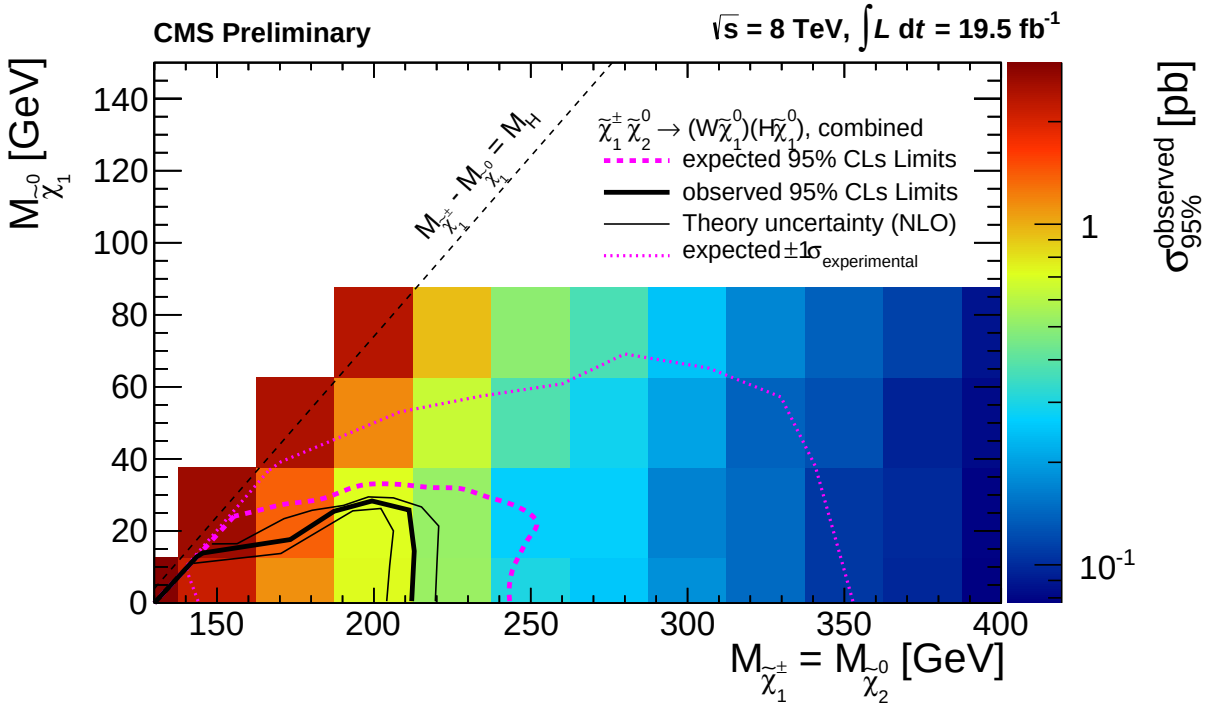

Figure 4: The interpretation of the combined results from the three search channels. The upper limit on the $\tilde{\chi}_1^{\pm}\tilde{\chi}_2^0$ production cross section is indicated in the color scale. The expected and observed regions for which the signal model is excluded reach from the origin to the solid red and solid black curve, respectively. The dashed red lines show the $\pm 1\sigma$ variations on the expected limit due to experimental uncertainties and the thin black lines indicate the uncertainty due to the cross section calculation.

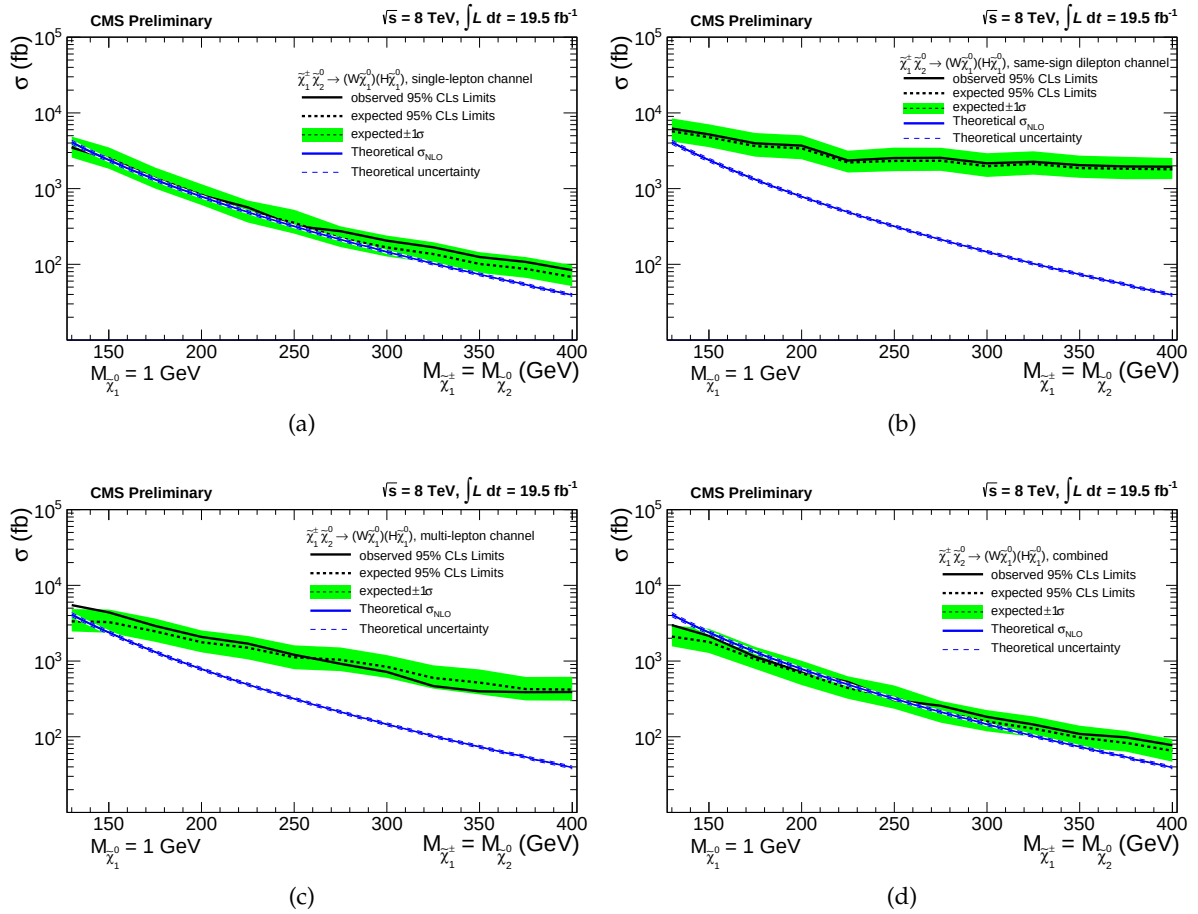

Figure 5: The interpretations of the results from (a) the single-lepton search, (b) the same-sign dilepton search, (c) the multi-lepton search, and (d) the combination of the three searches. The black curves show the expected (dashed) and observed (solid) limits on the $\tilde{\chi}_1^{\pm}\tilde{\chi}_2^0$ cross section times $\mathcal{B}(\tilde{\chi}_1^{\pm}\tilde{\chi}_2^0 \to \mathrm{WH} + E_{\mathrm{T}}^{\mathrm{miss}})$. The green band shows the $\pm 1\sigma$ variations on the expected limit due to experimental uncertainties. The solid blue curve shows the theoretical prediction for the cross section, with the dashed blue bands indicating the uncertainty on the cross section calculation.

References

[1] S. Dimopoulos and S. Raby, "Supercolor", *Nucl. Phys. B* **192** (1981) 353, doi:10.1016/0550-3213(81)90430-2.

[2] E. Witten, "Dynamical Breaking of Supersymmetry", *Nucl. Phys. B* **188** (1981) 513, doi:10.1016/0550-3213(81)90006-7.

[3] M. Dine, W. Fischler, and M. Srednicki, "Supersymmetric Technicolor", *Nucl. Phys. B* **189** (1981) 575, doi:10.1016/0550-3213(81)90582-4.

[4] S. Dimopoulos and H. Georgi, "Softly Broken Supersymmetry and SU(5)", *Nucl. Phys. B* **193** (1981) 150, doi:10.1016/0550-3213(81)90522-8.

[5] N. Sakai, "Naturalness in Supersymmetric Guts", *Z. Phys. C* **11** (1981) 153, doi:10.1007/BF01573998.

[6] R. K. Kaul and P. Majumdar, "Cancellation of quadratically divergent mass corrections in globally supersymmetric spontaneously broken gauge theories", *Nucl. Phys. B* **199** (1982) 36, doi:10.1016/0550-3213(82)90565-X.

[7] CMS Collaboration, "Search for new physics in events with same-sign dileptons and b-tagged jets in pp collisions at $\sqrt{s} = 7$ TeV", *JHEP* **1208** (2012) 110, doi:10.1007/JHEP08(2012)110, arXiv:1205.3933.

[8] CMS Collaboration, "Search for new physics in events with opposite-sign leptons, jets, and missing transverse energy in pp collisions at $\sqrt{s} = 7$ TeV", *Phys. Lett. B* **718** (2013) 815–840, doi:10.1016/j.physletb.2012.11.036, arXiv:1206.3949.

[9] CMS Collaboration, "Search for new physics with same-sign isolated dilepton events with jets and missing transverse energy", *Phys. Rev. Lett.* **109** (2012) 071803, doi:10.1103/PhysRevLett.109.071803, arXiv:1205.6615.

[10] CMS Collaboration, "Search for physics beyond the standard model in events with a Z boson, jets, and missing transverse energy in pp collisions at $\sqrt{s} = 7$ TeV", *Phys. Lett. B* **716** (2012) 260–284, doi:10.1016/j.physletb.2012.08.026, arXiv:1204.3774.

[11] CMS Collaboration, "Search for electroweak production of charginos and neutralinos using leptonic final states in pp collisions at $\sqrt{s} = 7$ TeV", *JHEP* **1211** (2012) 147, doi:10.1007/JHEP11(2012)147, arXiv:1209.6620.

[12] CMS Collaboration, "Search for electroweak production of charginos, neutralinos, and sleptons using leptonic final states in pp collisions at 8 TeV", CMS Physics Analysis Summary CMS-PAS-SUS-13-006, (2013).

[13] CMS Collaboration, "Observation of a new boson at a mass of 125 GeV with the CMS experiment at the LHC", *Phys. Lett. B* **716** (2012) 30–61, doi:10.1016/j.physletb.2012.08.021, arXiv:1207.7235.

[14] ATLAS Collaboration, "Observation of a new particle in the search for the Standard Model Higgs boson with the ATLAS detector at the LHC", *Phys. Lett. B* **716** (2012) 1–29, doi:10.1016/j.physletb.2012.08.020, arXiv:1207.7214.

[15] S. P. Martin, "A Supersymmetry primer", arXiv:hep-ph/9709356.

[16] CMS Collaboration, "A search for anomalous production of events with three or more leptons using 19.5 fb^{-1} of $\sqrt{s} = 8$ TeV LHC data", CMS Physics Analysis Summary CMS-PAS-SUS-13-002, (2013).

[17] T. Sjöstrand, S. Mrenna, and P. Z. Skands, "PYTHIA 6.4 Physics and Manual", *JHEP* **05** (2006) 026, doi:10.1088/1126-6708/2006/05/026, arXiv:hep-ph/0603175.

[18] J. Alwall et al., "MadGraph 5 : Going Beyond", *JHEP* **1106** (2011) 128, doi:10.1007/JHEP06(2011)128, arXiv:1106.0522.

[19] S. Frixione and B. R. Webber, "Matching NLO QCD computations and parton shower simulations", *JHEP* **0206** (2002) 029, arXiv:hep-ph/0204244.

[20] S. Frixione, P. Nason, and B. R. Webber, "Matching NLO QCD and parton showers in heavy flavor production", *JHEP* **0308** (2003) 007, arXiv:hep-ph/0305252.

[21] S. Frixione, P. Nason, and C. Oleari, "Matching NLO QCD computations with parton shower simulations: the POWHEG method", *JHEP* **11** (2007) 070, doi:10.1088/1126-6708/2007/11/070, arXiv:0709.2092.

[22] P. M. Nadolsky et al., "Implications of CTEQ global analysis for collider observables", *Phys. Rev. D* **78** (2008) 013004, doi:10.1103/PhysRevD.78.013004, arXiv:0802.0007.

[23] N. Kidonakis, "Differential and total cross sections for top pair and single top production", doi:10.3204/DESY-PROC-2012-02/251, arXiv:1205.3453.

[24] J. M. Campbell and R. K. Ellis, "$t\bar{t}W^{\pm}$ production and decay at NLO", *JHEP* **1207** (2012) 052, doi:10.1007/JHEP07(2012)052, arXiv:1204.5678.

[25] M. Garzelli, A. Kardos, C. Papadopoulos, and Z. Trocsanyi, " $t\bar{t}$ $W^{\pm}$ and $t\bar{t}Z$ Hadroproduction at NLO accuracy in QCD with Parton Shower and Hadronization effects", *JHEP* **1211** (2012) 056, doi:10.1007/JHEP11(2012)056, arXiv:1208.2665.

[26] J. M. Campbell and R. Ellis, "MCFM for the Tevatron and the LHC", *Nucl. Phys. Proc. Suppl.* **205-206** (2010) 10–15, doi:10.1016/j.nuclphysbps.2010.08.011, arXiv:1007.3492.

[27] R. Gavin, Y. Li, F. Petriello, and S. Quackenbush, "W Physics at the LHC with FEWZ 2.1", *Comput. Phys. Commun.* **184** (2013) 208–214, doi:10.1016/j.cpc.2012.09.005, arXiv:1201.5896.

[28] R. Frederix et al., "Four-lepton production at hadron colliders: aMC@NLO predictions with theoretical uncertainties", *JHEP* **1202** (2012) 099, doi:10.1007/JHEP02(2012)099, arXiv:1110.4738.

[29] P. Z. Skands et al., "SUSY Les Houches accord: interfacing SUSY spectrum calculators, decay packages, and event generators", *JHEP* **07** (2004) 036, doi:10.1088/1126-6708/2004/07/036.

[30] A. Djouadi, J.-L. Kneur, and G. Moultaka, "SuSpect: A Fortran code for the supersymmetric and Higgs particle spectrum in the MSSM", *Comput. Phys. Commun.* **176** (2007) 426–455, doi:10.1016/j.cpc.2006.11.009, arXiv:hep-ph/0211331.

[31] P. Meade and M. Reece, "BRIDGE: Branching ratio inquiry / decay generated events", arXiv:hep-ph/0703031.

[32] W. Beenakker et al., "Production of charginos, neutralinos, and sleptons at hadron colliders", *Phys. Rev. Lett.* **83** (1999) 3780, doi:10.1103/PhysRevLett.83.3780.

[33] W. Beenakker et al., "Erratum: production of charginos, neutralinos, and sleptons at hadron colliders", *Phys. Rev. Lett.* **100** (2008) 029901, doi:10.1103/PhysRevLett.100.029901.

[34] M. Krämer et al., "Supersymmetry production cross sections in pp collisions at $\sqrt{s} = 7$ TeV", (2012). arXiv:1206.2892.

[35] CMS Collaboration, "The fast simulation of the CMS detector at LHC", *J. Phys. Conf. Ser.* **331** (2011) 032049, doi:10.1088/1742-6596/331/3/032049.

[36] S. Agostinelli et al., "GEANT4 – a simulation toolkit", *Nucl. Instr. Meth. A* **506** (2003) 250, doi:10.1016/S0168-9002(03)01368-8.

[37] CMS Collaboration, "Study of tau reconstruction algorithms using pp collisions data collected at $\sqrt{s} = 7$ TeV", CMS Physics Analysis Summary CMS-PAS-PFT-10-004, (2010).

[38] CMS Collaboration, "CMS strategies for tau reconstruction and identification using particle-flow techniques", CMS Physics Analysis Summary CMS-PAS-PFT-08-001, (2009).

[39] CMS Collaboration, "Electron Reconstruction and Identification at $\sqrt{s} = 7$ TeV", CMS Physics Analysis Summary CMS-PAS-EGM-10-004, (2010).

[40] CMS Collaboration, "Performance of CMS muon reconstruction in pp collision events at $\sqrt{s} = 7$ TeV", *JINST* **7** (2012) P10002, doi:10.1088/1748-0221/7/10/P10002, arXiv:1206.4071.

[41] M. Cacciari, G. P. Salam, and G. Soyez, "The anti-k_t jet clustering algorithm", *JHEP* **04** (2008) 063, doi:10.1088/1126-6708/2008/04/063, arXiv:0802.1189.

[42] M. Cacciari and G. P. Salam, "Pileup subtraction using jet areas", *Phys. Lett. B* **659** (2008) 119, doi:10.1016/j.physletb.2007.09.077.

[43] CMS Collaboration, "Performance of τ lepton reconstruction and identification in CMS", *JINST* **7** (2012) P01001, doi:10.1088/1748-0221/7/01/P01001.

[44] CMS Collaboration, "Identification of b-quark jets with the CMS experiment", *JINST* **8** (2013) P04013, doi:10.1088/1748-0221/8/04/P04013, arXiv:1211.4462.

[45] CMS Collaboration, "Search for the standard model Higgs boson produced in association with W or Z bosons, and decaying to bottom quarks for LHCp 2013", CMS Physics Analysis Summary CMS-PAS-HIG-13-012, (2013).

[46] CMS Collaboration, "Search for top-squark pair production in the single-lepton final state in pp collisions at sqrt(s) = 8 TeV", arXiv:1308.1586. Submitted to *Eur. Phys. J. C*.

[47] Y. Bai, H.-C. Cheng, J. Gallicchio, and J. Gu, "Stop the Top Background of the Stop Search", *JHEP* **1207** (2012) 110, doi:10.1007/JHEP07(2012)110, arXiv:1203.4813.

[48] CMS Collaboration, "Search for new physics in events with same-sign dileptons and jets in pp collisions at 8 TeV", CMS Physics Analysis Summary CMS-PAS-SUS-13-013, (2013).

[49] C. Lester and D. Summers, "Measuring masses of semiinvisibly decaying particles pair produced at hadron colliders", *Phys. Lett. B* **463** (1999) 99–103, doi:10.1016/S0370-2693(99)00945-4, arXiv:hep-ph/9906349.

[50] A. Barr, C. Lester, and P. Stephens, "m(T2): The Truth behind the glamour", *J. Phys. G* **29** (2003) 2343–2363, doi:10.1088/0954-3899/29/10/304, arXiv:hep-ph/0304226.

[51] CMS Collaboration, "Search for new physics with same-sign isolated dilepton events with jets and missing transverse energy at the LHC", *JHEP* **1106** (2011) 077, doi:10.1007/JHEP06(2011)077, arXiv:1104.3168.

[52] A. L. Read, "Presentation of search results: The CL_s technique", *J. Phys. G* **28** (2002) 2693, doi:10.1088/0954-3899/28/10/313.

[53] T. Junk, "Confidence level computation for combining searches with small statistics", *Nucl. Instrum. Meth. A* **434** (1999) 435, doi:10.1016/S0168-9002(99)00498-2, arXiv:hep-ex/9902006.

[54] ATLAS and CMS Collaborations, LHC Higgs Combination Group, "Procedure for the LHC Higgs boson search combination in Summer 2011", ATL-PHYS-PUB/CMS NOTE 2011-11, 2011/005, (2011).

A Multilepton Analysis Additional Results

This section presents additional results tables for the multilepton analysis.

Table 4: Multi-lepton results for the $M_{\tilde{\chi}} = 150\,\text{GeV}, M_{\tilde{\chi}_1^0} = 1\,\text{GeV}$ model point. Details are the same as in Table 3.

$N_{\tau_{\text{had}}}$	OSSF pair	$E_{\text{T}}^{\text{miss}}$ [GeV]	Data	Total SM	Signal
0	below Z	50–100	142	125 ± 28	14.9 ± 2.8
0	below Z	100–150	16	21.3 ± 8.0	5.06 ± 0.86
0	none	0–50	53	52 ± 12	4.61 ± 0.99
0	none	50–100	35	38 ± 15	6.5 ± 1.1
0	none	100–150	7	9.3 ± 4.3	2.32 ± 0.43

Table 5: Multi-lepton results for the $M_{\tilde{\chi}} = 200\,\text{GeV}, M_{\tilde{\chi}_1^0} = 1\,\text{GeV}$ model point. Details are the same as in Table 3.

$N_{\tau_{\text{had}}}$	OSSF pair	$E_{\text{T}}^{\text{miss}}$ [GeV]	Data	Total SM	Signal
0	below Z	50–100	142	125 ± 28	4.90 ± 0.91
0	below Z	100–150	16	21.3 ± 8.0	2.63 ± 0.43
0	below Z	150–200	5	2.9 ± 1.0	0.61 ± 0.16
0	none	50–100	35	38 ± 15	2.31 ± 0.43
0	none	100–150	7	9.3 ± 4.3	1.31 ± 0.26

Table 6: Multi-lepton results for the $M_{\tilde{\chi}} = 300\,\text{GeV}, M_{\tilde{\chi}_1^0} = 1\,\text{GeV}$ model point. Details are the same as in Table 3.

$N_{\tau_{\text{had}}}$	OSSF pair	$E_{\text{T}}^{\text{miss}}$ [GeV]	Data	Total SM	Signal
0	below Z	100–150	16	21.3 ± 8.0	0.70 ± 0.13
0	below Z	150–200	5	2.9 ± 1.0	0.348 ± 0.067
0	below Z	> 200	0	0.88 ± 0.31	0.218 ± 0.041
0	above Z	150–200	1	2.48 ± 0.68	0.180 ± 0.045
1	none	150–200	8	15.1 ± 7.4	0.44 ± 0.12

Table 7: Multi-lepton results for the $M_{\tilde{\chi}} = 400\,\text{GeV}, M_{\tilde{\chi}_1^0} = 1\,\text{GeV}$ model point. Details are the same as in Table 3.

$N_{\tau_{\text{had}}}$	OSSF pair	$E_{\text{T}}^{\text{miss}}$ [GeV]	Data	Total SM	Signal
0	below Z	100–150	16	21.3 ± 8.0	0.167 ± 0.028
0	below Z	150–200	5	2.9 ± 1.0	0.138 ± 0.025
0	below Z	> 200	0	0.88 ± 0.31	0.137 ± 0.025
0	none	> 200	0	0.42 ± 0.22	0.057 ± 0.011
1	none	> 200	3	2.4 ± 1.1	0.152 ± 0.038